

Plasticization and Self Assembly in the Starch Granule

A. M. Donald¹**ABSTRACT**

Cereal Chem. 78(3):307–314

Within a starch granule there are a range of length scales present ranging from the atomic, to supramolecular structures of >100 nm that give rise to the growth rings arising as the starch is laid down. As the granule is formed, it is in a naturally hydrated state. This provides a degree of mobility permitting organization and self-assembly of the sidechain branches of the amylopectin. External factors that affect the ability of the

branches to pack well are discussed here. Plasticization of the residues nearest to the amylopectin backbone is crucial. If the degree of plasticization is insufficient (due to insufficient temperature or solvent) the double helical regions are disordered. Plasticization, this time of the amorphous growth rings, is also a necessary prerequisite for gelatinization.

There have been many studies of starch granule structure and these have used a wide variety of techniques. Microscopy (predominantly optical and scanning electron microscopy) is mainly used for looking at the whole granule. Such approaches have demonstrated the great diversity of granule sizes and shapes occurring naturally, ranging from the small granules of pea ($\approx 1\text{--}5\ \mu\text{m}$) to the much larger potato starch granules that can be as large as $80\text{--}100\ \mu\text{m}$. Cereal starches tend to be intermediate in size. Unusually, wheat has a bimodal distribution of granules with the small type being deposited later in the ripening of the cereal (Whistler et al 1984; Galliard and Bowler 1987).

Biochemical techniques have been extensively used to examine both the enzymes utilized in starch synthesis and also the make-up of the polysaccharides within the granule. Both amylose and amylopectin are very high molecular weight molecules; amylopectin is highly branched, whereas amylose is essentially linear. However, there are significant differences between the details of the macromolecules found in different species, both in average molecular weight, and in branch length distribution for the amylopectin (Hizukuri et al 1983; Koizumi et al 1991). The sidechain branches typically consist of 10–20 sugar residues.

X-ray scattering is another approach that has been frequently used. Wide-angle X-ray scattering (WAXS) has revealed the packing within the crystals of the granule, enabling a detailed analysis of the different polymorphs (Imberty et al 1987; Imberty and Perez 1988; Wang et al 1998). Cereal starches typically exhibit the A polymorph, whereas tubers show the B form and legumes the mixed state polymorph C. WAXS essentially deals with interatomic distances. Less extensively used is small-angle X-ray scattering (SAXS) which, due to the reciprocal relationship between spacings in real space and in the scattering pattern, probes larger length scales than WAXS (those corresponding to supramolecular packing). Starch granules show a characteristic peak in the SAXS pattern corresponding to a repeat of $\approx 9\ \text{nm}$, at a so-called q spacing (q represents angular distance in the scattering pattern) of $\approx 0.62\ \text{\AA}^{-1}$. A single small-angle peak is often observed in semicrystalline polymeric systems. In this case, it is deemed to be the result of a particularly distorted periodic arrangement of amorphous and crystalline regions in the polymer, so that higher order reflections are not seen as would be the case for a more regular structure. In general, the requirements for observing a small-angle scattering peak are both periodicity (though it can be of an extremely distorted nature) and sufficient contrast in scattering length or electron densities between regions of the periodicity. In this review,

we explore conditions that permit the peak to be observed, looking at changes that can affect both of the required conditions for the peak to be seen.

Gelatinization, that process by which the internal structure of the granule is broken down and the whole granule disintegrates, releasing the polysaccharides into the surrounding medium, is accompanied by a variety of changes. Being semicrystalline, the granule exhibits birefringence when viewed between crossed polars. As the starch granules gelatinize and the structure is disrupted, this birefringence is lost. Whereas the loss of birefringence occurs over quite a large temperature range for the whole sample (Hill and Dronzek 1973), individual granules are observed to lose birefringence over a much smaller range, generally $<1^\circ\text{C}$ (French 1984). Substantial swelling occurs during the gelatinization process. This can be observed readily by optical microscopy. Information on granule swelling can also be obtained from thermomechanical analysis (TMA). Swelling curves measured for rice starch heated at $2^\circ\text{C}/\text{min}$ and compared with differential scanning calorimetry (DSC) curves suggest the same qualitative conclusion (Biliaderis 1986). It should be noted, however, that granule swelling may not occur uniformly in all granule dimensions. Scanning electron microscopy (SEM) studies on the changing shape of wheat starch granules during gelatinization (Bowler et al 1980) observed a highly anisotropic two-stage swelling process.

Loss of crystallinity also occurs at the same time as these macroscopic changes during gelatinization, as demonstrated by WAXS. Crystallinity loss has been quantitatively correlated with thermal events (as measured by DSC) in a detailed study by Liu et al (1991), and more recently by Jenkins and Donald (1998). A similar investigation was made by Cooke and Gidley (1992) with the additional use of NMR to measure double helix content. They observed that crystalline and molecular order are lost concurrently during gelatinization. Further work included measurement of birefringence loss (Gidley and Cooke 1991). Birefringence loss started earlier and concluded earlier than molecular and crystalline order loss (Liu et al 1991).

Using SAXS and WAXS simultaneously during gelatinization in water, together with small angle neutron scattering (SANS), it has been possible to probe the processes that occur at both the molecular and supramolecular length scales. SANS explores events on distances similar to SAXS but is sensitive to differences in the nuclei off which the neutrons scatter (Jenkins and Donald 1998). It is possible to explore the distribution of water within the granule as gelatinization proceeds by using mixtures of water and heavy water (H_2O and D_2O) because the deuterium nucleus has a very different scattering length density from that of hydrogen. These multitechnique studies have suggested the following steps occur during gelatinization in excess water. First, the macroscopic swelling observed at early stages in the gelatinization process is associated with water ingress into the amorphous growth rings. The semicrystalline lamellae themselves do not expand radially, so overall periodicity revealed by the

¹ Cavendish Laboratory, Madingley Road Cambridge CB3 0HE, UK. E-mail: amd3@phy.cam.ac.uk

9-nm peak is unchanged. Crystallinity, measured by the crystallinity index (Wakelin et al 1959), includes a contribution from helical regions of the amylopectin sidechains and is principally, but not exclusively, lost during the DSC gelatinization endotherm. It seems that some residual double helix component remains after the longer range correlations within crystals are lost. Redistribution of water in the semicrystalline lamellae only occurs at a comparatively late stage.

As a consequence of these processes, as postulated by Donovan (1979), gelatinization is primarily a swelling-driven process. The initial water uptake occurs in the amorphous growth ring and is accompanied by swelling within this region without radial expansion of the semicrystalline lamellar region. However, the amylopectin molecules at the edges of the lamellar stack must also form bonds with the amorphous regions, leading to a coupling of the semicrystalline regions with the amorphous regions. Thus, as swelling occurs within the amorphous regions, a stress is imposed on the amylopectin crystallites. The buildup of this stress causes the amylopectin double helices within the crystallites to dissociate, first from neighboring double helices and, subsequently, by unwinding. This process occurs rapidly for an individual crystallite, but over a

wide temperature range for the whole granule. Smaller crystallites are less stable and are destroyed first. This swelling-driven crystallite disruption process gives rise to the G endotherm observed in DSC studies of starch gelatinization in excess water (Donovan 1979).

If gelatinization takes place in a medium other than excess water, the DSC curves show changes. If solutes such as sugar are present in the water, the gelatinization endotherm shifts to higher temperature, and these shifts can be substantial. The second part of this review considers how this mechanism is altered in sugar solutions. Plasticization again plays a crucial role in rationalizing the processes.

MATERIALS AND METHODS

DSC

A Perkin Elmer DSC-7 equipped with an Intracooler II was used at a heating rate of 10°C/min. An empty sample pan was used as a reference. Samples were made up as starch slurries of varying composition and were sampled in one of two forms of sample pan. The solutes studied were glycerol and glucose. For samples that were not heated to >100°C, where the risk of solvent loss was usually low, scans were performed using standard aluminum 40- μ L sample pans. In cases where the temperature of interest passes this point, Perkin Elmer large volume capsules (LVC) were used. The LVC had an internal volume of 60 μ L and could withstand internal pressures of up to 240 atm, hence, the possibility of water loss, even at elevated temperatures was significantly reduced. Data were analyzed with Perkin Elmer system software. Sample masses were 10–25 mg.

SAXS/WAXS

The simultaneous SAXS/WAXS experiments described in this study were performed on station 8.2 at the Synchrotron Radiation Source at the Daresbury Laboratory, UK. All experiments described were conducted with the small-angle detector camera length set at 1.5–3.5 m. The small-angle gas-filled quadrant detector is multiwire and produces powder averaged diffraction data. The wide-angle Inel detector measures powder averaged scattering using a single delay line.

Samples were made up as starch slurries of \approx 40–45% (w/w) starch in general. Starch slurries (63%) were used for the limiting solvent conditions. Waxy maize and potato starch were both gifts from

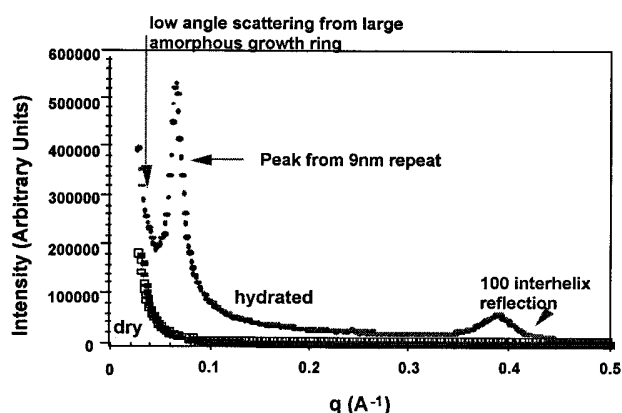


Fig. 1. Small-angle X-ray scattering (SAXS) curves for hydrated (●) and dehydrated (■) potato starch showing 9-nm peak and 100 interhelix peak at larger angle. Dehydrated starch \approx 5% moisture overall. q = Angular distance in the scattering pattern.

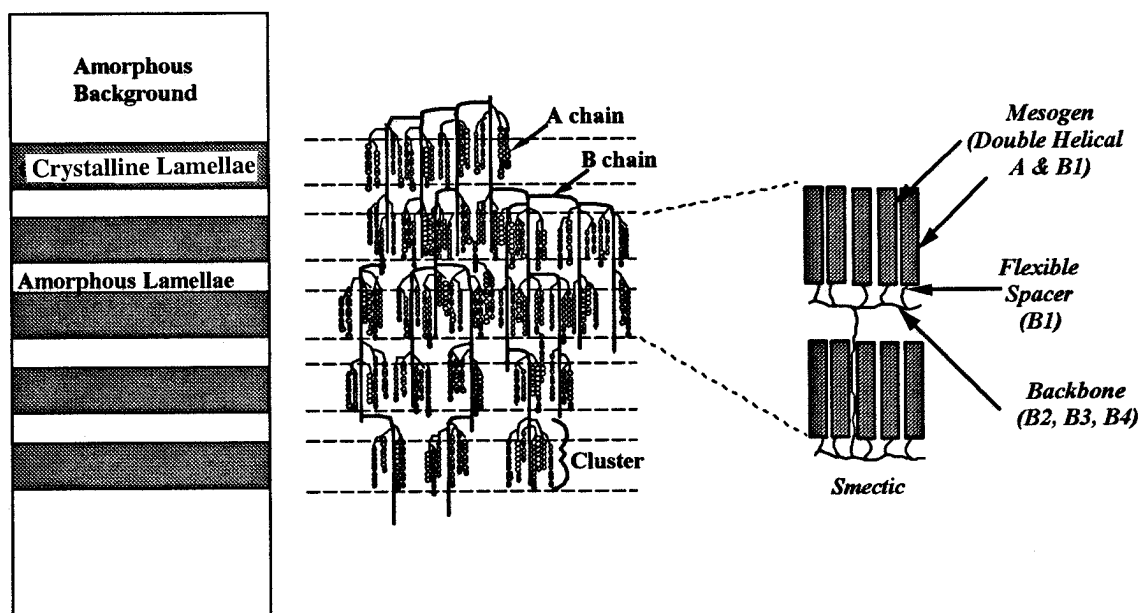


Fig. 2. Starch granule semicrystalline stack embedded in an amorphous growth ring (left); amylopectin cluster with double helices packed into lamellar structure (center); same part of the amylopectin molecule using the language of sidechain liquid crystalline polymers (right). Double helices are mesogens attached to the backbone of amylopectin chain through flexible spacers.

National Starch. Solutions of glycerol were made up with simple stirring, while solutions of glucose were made by combining stirring and heating. Samples were placed in aluminum DSC pans supplied by TA instruments. These pans were modified in an attempt to avoid strong absorption of X-rays by aluminum. Additional details about the design of the pan and beamline can be found elsewhere (Bras et al 1995).

All SAXS/WAXS data were reduced as described previously (Cameron and Donald 1992; Jenkins et al 1994; Jenkins and Donald 1998). Fitting procedures to extract appropriate parameters from the SAXS curves have been fully discussed elsewhere (Cameron and Donald 1992). The WAXS data has been analyzed using the Wakelin method (Wakelin et al 1959) to describe the crystallinity index as described previously (Jenkins et al 1994; Jenkins and Donald 1998).

SANS

SANS experiments were conducted on the LOQ beamline at the ISIS spallation neutron source at the Rutherford Appleton Laboratory in Didcot, UK. Samples were prepared according to the method of Jenkins and Donald (1996). The possibility of H-D exchange occurring during experimentation was eliminated by preequilibration of vacuum-dried starch samples in water of the appropriate composition. Waxy maize starch was a gift from National Starch and Chemical Co.

After preparation, starch samples were made up to 40% (w/w) starch in water or glycerol, composed of 100, 90, 80, 50, 10, and 0% (molar basis) H₂O or deuterated glycerol, before injecting into circular quartz sample cells of 1- or 2-mm path lengths. Further details of sample preparation and the analysis used can be found in Jenkins and Donald (1996) and Perry and Donald (2000a,b).

RESULTS

Self Assembly

In hydrated B-type starch-water systems, two peaks are seen in the small angle X-ray scattering profiles (Fig. 1). Neither of these peaks is present in the diffraction patterns of dry starch. (In this case, the sample was vacuum-dried for one day. It probably contains water levels of ≈5%, w/w). For A-type cereal starches, a similar loss of the 9-nm peak upon dehydration also occurs, but it cannot be correlated with the interhelix behavior because the 100 interhelix peak is never seen (it is a systematic absence for the A-type crystal structure). The presence of a peak in the SAXS pattern is attributed to the

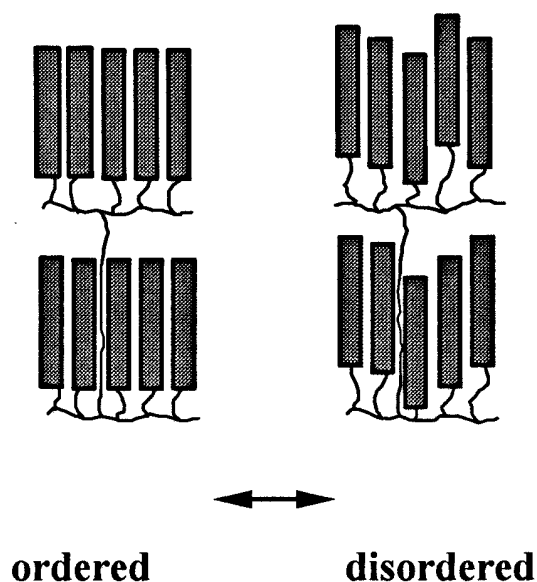


Fig. 3. Transition between ordered (smectic) and disordered (nematic) structure for double helical regions. Transition can go in either direction.

existence of a periodicity, even if distorted, and sufficient contrast in scattering length and electron densities between the regions of the periodicity (in this case, the semicrystalline lamellar stack).

The model used to discuss the SAXS curves has been well documented (Cameron and Donald 1992; Jenkins et al 1993). It assumes a stack of semicrystalline lamellae embedded in amorphous growth rings. Amorphous growth rings were observed in etched granules in the scanning electron microscope (Buttrose 1962, 1963; Yamaguchi et al 1979; Atkin et al 1998). The separations are >100 nm and of so large a periodicity, they give rise to the upturn in scattering at low-scattering vector q (Fig. 1). A schematic view of the lamellar stack and surrounding amorphous growth ring is shown in Fig. 2. Within the crystalline lamellae, the crystals are formed from double helix formation of the amylopectin sidechain branches (Robin et al 1975; Blanshard 1987). The existence of the 9-nm repeat visible in Fig. 1 lies in a regularity in the spacing and appears to be universal, regardless of the species of starch (Jenkins et al 1993).

Also shown in Fig. 2, is an alternative way of representing the packing of the double helices, using the framework derived for synthetic sidechain liquid crystalline polymers (Donald and Windle 1992). In this parlance, the double helix units are known as mesogens, which are rigid units that tend to align. The lamellar crystals are equivalent to layers of smectic packing. For the double helices to be able to align, it is necessary that they are not attached too rigidly to the amylopectin backbone. The segment of sidechain that decouples the helical forming unit from the backbone is the flexible spacer. The spacer units are necessarily amorphous and flexible due to the relative flexibility of both the $\alpha(1\rightarrow4)$ and $\alpha(1\rightarrow6)$ linkages (Buleon and Tran 1990) and their inability to form a stable single helix. Figure 2c shows the labeling of the different parts of the amylopectin with both the standard identifications used for amylopectin (Hizukuri 1986) and for liquid crystalline polymers. Using the language of liquid crystalline polymers helps understand the change between the dry and hydrated state in the scattering pattern shown in Fig. 1.

The original explanation for the disappearance of the 9-nm peak upon dehydration was that it was due to a lack of contrast, (contrast is one of the two requirements for a peak to be visible). However, it is not possible to see how this could also affect the 100 interhelix peak in the B-type pattern shown in Fig. 1.

Instead, the underlying cause for the simultaneous disappearance of both peaks must lie in some change in packing removing the

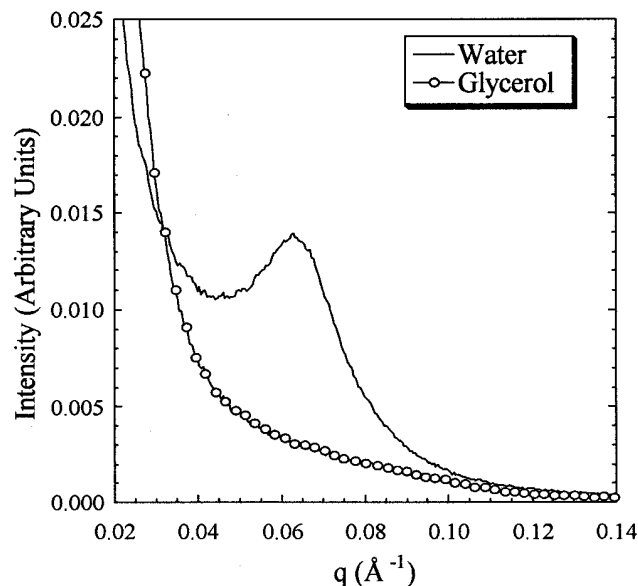


Fig. 4. Room temperature small-angle X-ray scattering (SAXS) curves for waxy maize in pure water (solid line) and pure glycerol (—○—). q = Angular distance in the scattering pattern.

long-range correlations between the layers and also the lateral packing of the double helices. As Fig. 2c shows, there is smectic organization in layers between the lamellar crystals. If the layers are disrupted, then the 9-nm peak will be lost, as well as the register between double helices. Figure 3 shows this transition. The packing is still lamellar-like but much less ordered than before. This type of packing is known in the liquid crystal field as nematic.

It is straightforward to rationalize why dehydration might have this effect. In the dry state, it is postulated that the helices are intact (WAXS data indicates considerable crystallinity in the dry sample) but are not arranged regularly side by side. The so-called flexible spacers are no longer as flexible as they were when there was plenty of water around, and now the differing lengths of the amorphous chains to which they are attached pull them apart. The balance has shifted so that the entropy of the backbone, which favors disorder, overcomes the tendency of the enthalpic interactions between double helices to promote order. The key change to amylopectin molecules upon dehydration is that the degree of plasticization of the flexible spacer has decreased.

At room temperature, under standard conditions of moisture, all starches show the 9-nm peak. However, if the starch is placed in other solvents, the SAXS pattern resembles the dry starch. Thus, the granules may be surrounded by excess solvent such as glycerol, and yet the packing of the double helices is not good enough for the scattering to show the 9-nm peak. Figure 4 shows a comparison of the behavior of waxy maize at room temperature when dispersed in water and glycerol. The SAXS curve for starch in glycerol at room temperature resembles the dry state of the starch: no 9-nm peak is visible. Thus, if the rationale for the absence of the peak in dry starch is insufficient plasticization and flexibility of the flexible spacer, is this the same answer for the starch in glycerol?

To verify that this is not an issue of contrast (perhaps the glycerol in the amorphous lamellae makes these regions sufficiently electron dense that there is no longer any difference in scattering properties with the crystalline lamellae), small angle neutron scattering experiments were conducted using deuterated glycerol. By changing the H/D ratio, one can change the scattering length density (and hence contrast for the neutrons), if in 100% hydrogenated glycerol there happened to be no contrast, this should not apply in other compositions of the solvent. Figure 5 shows that, whatever the composition of the glycerol in terms of H/D ratio, the scattering pattern is

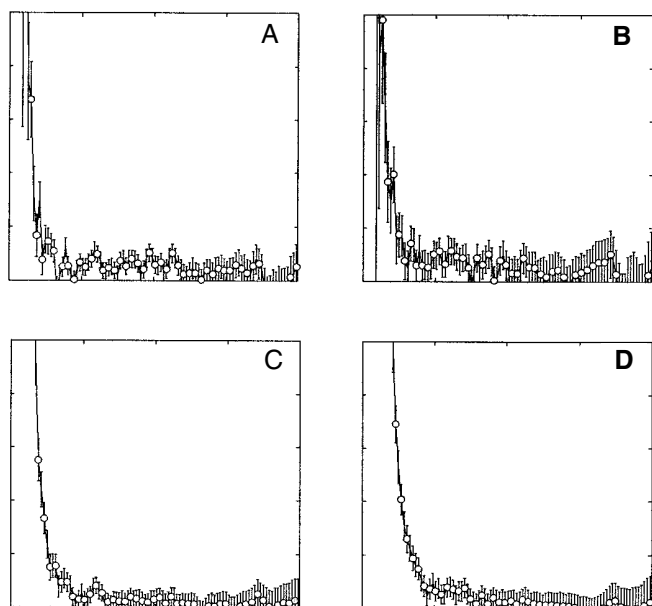


Fig. 5. Small-angle neutron scattering (SANS) curves for waxy maize starch in glycerol at room temperature at four ratios. Molar percentages of H-glycerol used: A) 100%, B) 80%, C) 20%, D) 0%.

essentially unchanged. This data is for waxy maize, as it is the strongest scatterer of the starches, but SANS data are always much noisier than corresponding SAXS curves because the flux at the neutron source is much lower than at a synchrotron source for X-rays. From Fig. 5, we can again eliminate lack of contrast as the explanation. The periodicity must be absent under these conditions.

However a very different scattering curve is obtained at elevated temperature. Figure 6 shows a superposition of curves for different glycerol contrasts for waxy maize at 85°C. At this temperature a peak is seen, but its height varies with the composition of the glycerol. Clearly contrast does affect the magnitude of the peak, and at 80% H-glycerol, the contrast between the crystalline and amorphous lamellae does indeed vanish (this is known as the contrast match point) (Higgins and Benoit 1996). But at compositions with either more or less deuterium in the glycerol, the peak is visible. From the variation in peak height with H/D ratio, it is in principle possible to quantify the amount of solvent distributed between the different phases (Jenkins and Donald 1996; Perry and Donald 2000a,b), but this is beyond the scope of this review. For the present, we need to establish what the consequences of temperature are for this particular solvent.

DSC curves give a further clue as to how the packing is changing in glycerol as a function of temperature. In this case, hydrogenated glycerol is used throughout, but small amounts of water have been added to the glycerol (glycerol and water are miscible over the entire composition range). Figure 7 shows the results for concentrated glycerol solutions. It is possible to see an exotherm occurring in solutions of >80% glycerol. The temperature at which this occurs, indicated by arrows, depends on the glycerol concentration, moving upward in temperature as the glycerol concentration increases. This exotherm (which corresponds to heat being given out) occurs significantly below the temperature at which the more familiar gelatinization endotherm occurs. The position of this endotherm is, as with all sugar solutions, also a function of concentration and shifts upward markedly as the solute concentration in an aqueous solution increase (Blanshard 1987). The presence of the lower temperature exotherm indicates that some transition is occurring which leads to an altered state of organization and, hence, the release of energy.

Figure 8 shows the corresponding changes in the SAXS pattern when waxy maize in a concentrated glycerol solution (90%) is heated. At room temperature (as shown in Fig. 4), the 9-nm peak is not present, but it grows as the temperature is raised to >40°C, the increase flattening off at >51°C. This corresponds to the temperature at

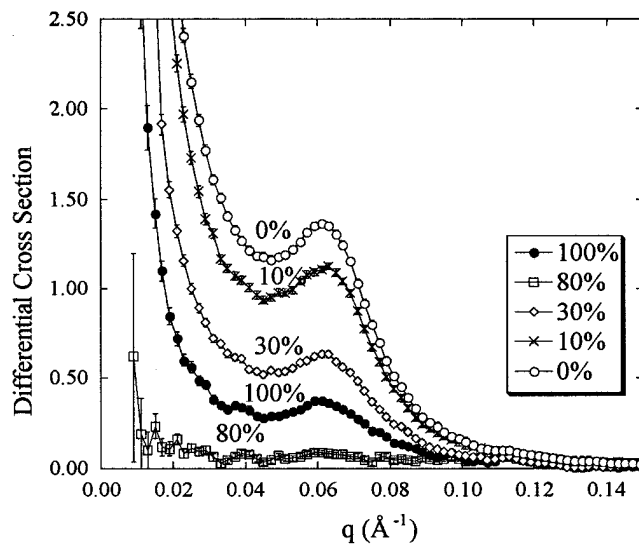


Fig. 6. Small-angle neutron scattering (SANS) curves for waxy maize starch in glycerol at 85°C. Different proportions of hydrogenated glycerol are used for the solvent. Numerical values give molar percentage of H-glycerol used. q = Angular distance in the scattering pattern.

which the exotherm is seen in the DSC traces for solutions of this composition (Fig. 7). Similar correlations can be made between the temperature at which SAXS curves for all the glycerol concentrations flatten off with the exotherm revealed by DSC, as shown in Fig. 9. The plot shows how the 9-nm peak intensity increases with temperature, together with (vertical lines) the temperature of the DSC exotherm for that concentration of glycerol. There is a very strong correlation: the exotherm arises from the reordering associated with the lamellar structure organizing to give rise to long-range correlations.

We can conclude from these observations that, whereas at room temperature the flexible spacers are insufficiently plasticized in concentrated glycerol solutions to give rise to smectic ordering, as the temperature is raised, solvent ingress and accompanying plasticization and enhanced mobility permit the transition shown in Fig. 3, from right to left. Glycerol is a substantially larger molecule than water, and it is not surprising that it enters the granule with more difficulty (requiring higher temperatures) than water. For low glycerol concentrations in water, the exotherm is not seen in DSC, and the SAXS patterns always exhibits the 9-nm peak.

In summary, although a naturally hydrated granule exhibits a high degree of correlation between the crystalline lamellar crystals, under other conditions, a less organized state of packing exists. To facilitate this improvement in order, the so-called self assembly of the lamellae, a sufficient degree of plasticization by an appropriate small molecule is required. This molecule need not be water, as is seen by the example of glycerol. However, other sugar solutions and polyols behave in qualitatively the same way, although each system has a different temperature dependence. For self assembly to proceed, the plasticizer must be able to enter the granule. The ease with which this is able to occur will depend on molecule size, as well as factors such as the possibility of specific interactions between solvent and starch (such as hydrogen bonding) and the diffusion coefficient. Properties of the starch granule itself may affect the latter, so different starches show quantitatively different responses. For instance, potato starch, which is known to possess rather dense amorphous regions that will impede ingress of small molecules, only self assembles at temperatures some tens of degrees higher than the corresponding case for waxy maize in glycerol solutions (Perry and Donald 2000a,b)

Gelatinization

The data in Fig. 7 shows the gelatinization endotherm in glycerol solutions increases, as does the self-assembly exotherm, as the concentration of glycerol increases. We have just seen that the latter in-

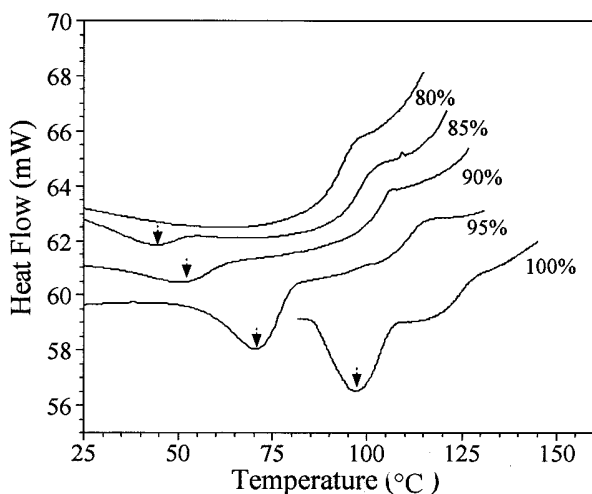


Fig. 7. Differential scanning calorimetry (DSC) traces, vertically offset, from waxy maize starch heated at 10°C/min in aqueous glycerol and water solutions of 80, 85, 90, 95, and 100% (w/w). Arrows mark position of exotherm (reprinted with permission).

creases due to the requirement of sufficient plasticization. We will now examine whether this same hypothesis serves to explain the behavior during gelatinization.

Figure 10 shows how the temperature of the gelatinization endotherm shifts with solution concentration for aqueous solutions of glycerol and glucose. However, as Fig. 7 showed, the endotherm itself does not change shape. Unlike limiting water, when the gelatinization endotherm shifts upward and broadens and ultimately splits into two (Donovan and Mapes 1980), there is no indication that splitting or broadening occurs in these high-solute systems. Changing the concentration of starch to solute also does not lead to a broadening or splitting of the endotherm, as long as the overall solvent concentration is sufficiently high (Perry 1999).

From the SAXS data, it is possible to extract more quantitative information about the changes that occur during gelatinization. Using the model described elsewhere (Cameron and Donald 1992), we can extract information from the data on the electron density differences between the three regions identified within the granule. The amorphous and crystalline lamellae, and the amorphous growth ring, furthermore, follow the changes in these differences as gelatinization proceeds. Figure 11a shows data for the temperature variation of $\Delta\rho_u = \rho_u - \rho_a$, where ρ_u and ρ_a are the electron densities of the amorphous growth ring and amorphous lamellae, respectively. For pure water, as gelatinization proceeds, water enters the amorphous growth ring first, causing swelling to occur before disruption of the crystallites (Jenkins and Donald 1998). For this situation, $\Delta\rho_u$ starts to decrease around the onset of the gelatinization endotherm with a maximum change in slope at the peak temperature (vertical dashed line in Fig. 11). The same qualitative behavior is observed for glycerol solutions of different concentrations as for pure water, suggesting that an identical mechanism for gelatinization is occurring, apart from the upward shift in gelatinization behavior. As with the DSC data, there is no indication that the high glycerol concentration is equivalent to the condition of limiting water. If other indicators obtainable from simultaneous SAXS/WAXS are considered ($\Delta\rho = \rho_c - \rho_a$, where ρ_c is the electron density of the crystalline lamellae, or the crystallinity index which can be determined from the WAXS data), then the same conclusion is drawn: glycerol and water solutions behave the same way.

This behavior can be contrasted with limiting solvent conditions, be it of water or glycerol. If the behavior of $\Delta\rho_u$ for starch in excess and limiting conditions are compared (Fig. 11b), a clear difference can be seen in the shape of the curves (excess solvent conditions in this graph correspond to 40% starch, limiting solvent to 63% starch).

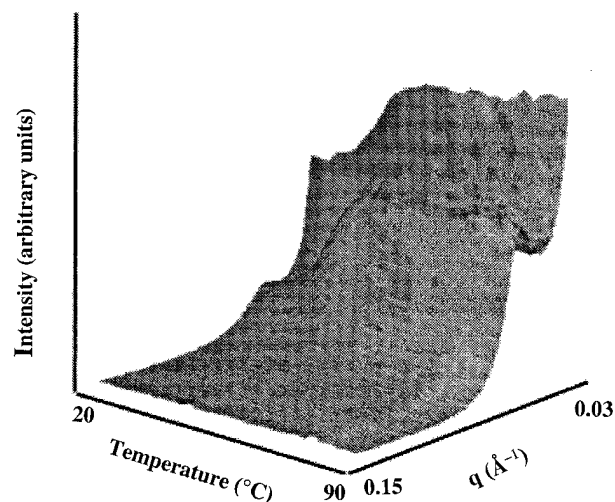


Fig. 8. Dynamic small-angle X-ray scattering (SAXS) data from waxy maize starch heated at 2°C/min in 90% glycerol solution. Note 9-nm peak at $\approx 52^\circ\text{C}$.

In line with what is known about the shape of the DSC curves in limiting water (Donovan and Mapes 1980), the slope of the $\Delta\rho_u$ curves has a discontinuity indicating an underlying two-step process and a consequent broadening of the transition region. This behavior applies to both pure water and 40% glycerol under limiting conditions. Thus, we can see that the upward shift in the gelatinization behavior in glycerol (and other sugar solutions) (Perry 1999) does not necessarily occur as a consequence of meeting limiting conditions. If the starch-to-solvent ratio is low and excess solvent is present, the mechanism is quite distinct from limiting conditions, regardless of the type of solvent. If the starch content is high, again similar behavior is seen whether the solvent is water or glycerol.

Earlier in this review, we saw how plasticization of the lamellae is hindered in solvents other than water (their ingress is less easy). More generally this means that, at a given temperature, less glycerol than water enters all parts of the granule. For gelatinization to occur, we know that much water must enter the amorphous growth ring and plasticize and swell it before crystal disruption can occur and gelatinization is completed (Jenkins and Donald 1998). It follows that the temperature for glycerol solutions to gelatinize is higher

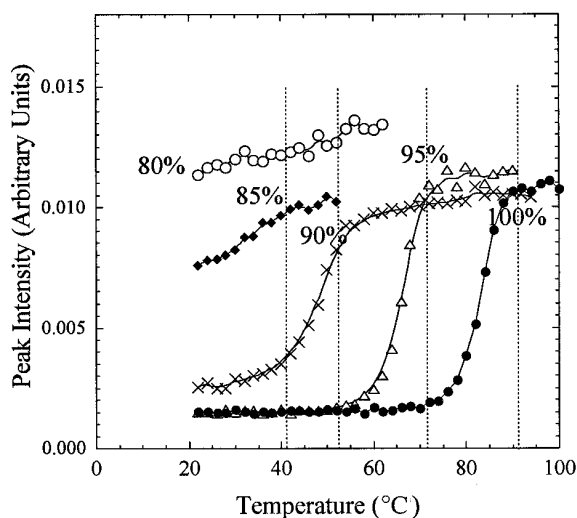


Fig. 9. Variation in small-angle X-ray scattering (SAXS) peak intensity ($q_{\text{peak}} = 0.064 \text{ \AA}^{-1}$) from waxy maize starch heated at $2^\circ\text{C}/\text{min}$ in concentrated (80–95%) glycerol in water solutions and pure glycerol (100%). Vertical lines mark peak temperatures of exothermic transitions determined by differential scanning calorimetry (DSC) for the four highest concentrations of glycerol. No exotherm is detectable for the 80% solution (reprinted with permission).

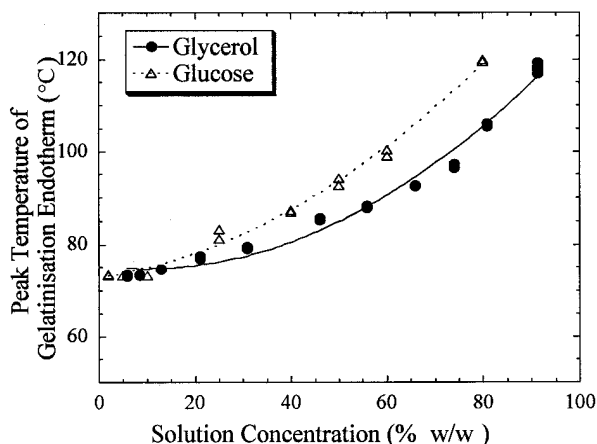


Fig. 10. Peak temperatures of waxy maize starch gelatinization as a function of glycerol and glucose concentration at a heating rate of $10^\circ\text{C}/\text{min}$.

than for water. A rationale, in terms of overall levels of plasticization can therefore be proposed for the familiar raising of gelatinization temperature in sugar solutions.

Pulling these findings together, we propose that gelatinization is initiated at the point at which the degree of molecular mobility within the amorphous growth ring regions is sufficient. Molecular mobility in these regions will be controlled by the total degree of plasticization induced by a combination of the input of plasticizing solvent and thermal energy. The point at which gelatinization is initiated can thus be thought of as the limiting point of stability on a plasticization curve. At this critical point, the mobility and swelling of the amorphous growth ring regions reaches a maximum level, beyond which native granular structure is irreversibly altered. The uptake of solvent upon swelling of the amorphous growth rings

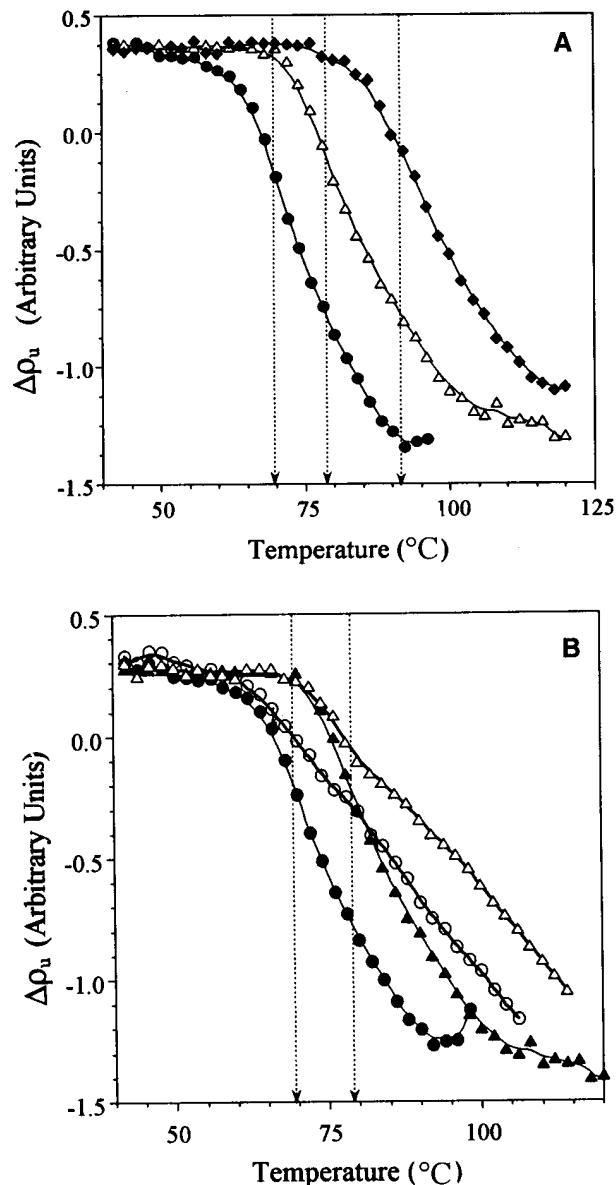


Fig. 11. **A,** Temperature dependence of $\Delta\rho_u$ for waxy maize starch in solutions of pure water (●) and glycerol (Δ 40%, \blacklozenge 70%) and water mixtures under conditions of excess solution with 40% starch. Vertical lines represent peak temperatures of differential scanning calorimetry (DSC) endotherm for three systems. **B,** Temperature dependence of $\Delta\rho_u$ for waxy maize starch in solutions of pure water in excess (●) and limiting (○) conditions; and a 40% glycerol and water mixture under excess (\blacktriangle , 40%) and limiting (Δ , 64%) conditions. Vertical lines correspond to peak temperature of DSC endotherm in excess pure water (left) and excess 40% glycerol (right).

leads to a cooperative cycle of increasing plasticization, molecular mobility, and structural disruption.

It is proposed that the critical degree of plasticization, molecular mobility, and swelling that are necessary to initiate gelatinization is the same regardless of the plasticizing solvent. The less effective the solvent is at plasticizing the granule, the greater the amount of thermal plasticization necessary to bring the total level of molecular mobility within the amorphous growth rings to the stability apex of the plasticization curve. Essentially the same logic applies to the lower temperature process of self assembly already discussed. This hypothesis can be considered as an amalgamation and extension of the ideas of Waigh (1997), Slade and Levine (1989), Donovan (1979), and Jenkins (1995). The ideas of Slade and Levine on the importance of plasticization and mobility in initiating gelatinization is placed on a solid structural basis. The site of plasticization is made explicit as the amorphous growth rings, followed by swelling-driven crystallite disruption (Jenkins and Donald 1998).

The influence of solvent levels on gelatinization can also be explained in terms of the idea of a continuous plasticization-mobility curve, building on the idea of Slade and Levine of a mobility map. In excess solvent, cooperative swelling and solvent uptake results in the complete disruption of lamellar and crystalline order by the swelling-driven crystallite disruption mechanism described. A single endotherm is observed in DSC traces, arising from the granular disruption brought about by the cooperative combination of increasing solvent and thermal plasticization and the molecular mobility and swelling that this induces.

As the relative amount of solvent is reduced to limiting solvent levels, systems initially begin to gelatinise by the same process as in excess solvent. However, once all of the available solvent external to the granule has been exhausted, the cooperative plasticization process is arrested. Further gelatinization is dependent on increased levels of molecular mobility and granular swelling, which can only be brought about by the input of thermal energy. Samples must therefore be heated to temperatures higher than in excess solvent, leading to the biphasic nature of gelatinization in limiting solvent and the broadening of the gelatinization temperature range.

It is clear that water is in no way unique in the way it interacts with the granule. Polyols such as glycerol behave in qualitatively the same way, but because they are less effective as plasticizers either for the lamellar regions or the amorphous growth ring, a higher temperature is required to permit an equivalent degree of plasticization and mobility. These ideas show how it is possible to unify the response of a variety of systems under different solvent conditions. The ideas presented here will be equally applicable to conditions under which starch is processed to make it a viable thermoplastic (Tomka 1991; Simmons et al 1992). This analysis can therefore help to rationalise the conditions that need to be present in an extruder to permit complete disintegration of the granules to make a viable plastic material.

CONCLUSIONS

This review demonstrates that understanding the interaction of solvents with the different parts of the starch granule enables us to construct a coherent picture to explain many different phenomena. Key to this understanding is realising that water is not unique in the way it interacts with starch. However, it does enter the granule more easily than any other solvent and therefore provides a baseline against which other solvents can be compared.

The well-known 9-nm repeat in the supramolecular packing of starch granules, arising from the periodicity in the semicrystalline lamellae, can only form if there is sufficient mobility of the amylopectin sidechain branches to enable the double helices, which form the basis of the crystalline lamellae, to order despite their attachment to the amylopectin backbone. In the absence of sufficient plasticization of these flexible spacers, the double helices pull out of registry and the 9-nm peak is lost. At room temperature, this lack

of order prevails both in dry (and therefore obviously unplasticized granules), but also for granules dispersed in other solvents such as sugar and polyol solutions. In the latter solutions, thermal energy has to be added to the slurries before sufficient mobility and plasticization occurs for the transition to the ordered smectic phase to occur. When the transition does occur, an exotherm is seen in the DSC traces at a temperature that correlates with the appearance of the 9-nm peak in the SAXS pattern. How much thermal energy has to be added depends both on the nature of the solvent and the type of starch used because not all granules are equally easily penetrated.

Once the self-assembly of the lamellar structure has occurred, further heat is required before gelatinization can proceed. Gelatinization is driven by ingress of solvent into the amorphous growth ring regions of the granule, accompanied by swelling and enhanced mobility. As more and more solvent enters the granule, a point will be reached at which sufficient mobility is imparted to the amorphous regions that they impose stresses onto the lamellar crystals and start their destruction. This corresponds to gelatinization. Again, it is the efficiency of the particular solvent and the nature of the type of granule used which will determine how much upward shift there is in the gelatinization temperature compared with pure water. Whatever the solvent, as long as the starch concentration is sufficiently low so as not to enter limiting solvent conditions, the mechanism of gelatinization is unchanged. The only change is the upward shift in temperature without any broadening of the endotherm associated with the process.

ACKNOWLEDGMENTS

This work builds on the PhD theses of Thomas Waigh and Paul Perry, to whom I am indebted. Their input was always stimulating and much appreciated. Funding for their work came primarily from the BBSRC, with additional support from Unilever, plc and Nestle. Access to the facilities at Daresbury, Warrington, UK, and Rutherford Appleton Laboratory are gratefully acknowledged, along with the help of Ernie Komanshek and Richard Heenan, respectively.

LITERATURE CITED

- Atkin, N. J., Abeysekera, R. M., and Cheng, S. L. 1998. An experimentally-based predictive model for the separation of amylopectin subunits during starch gelatinization. *Carbohydr. Polym.* 36:173.
- Biliaderis, C., Page, C., and Maurice, T. 1986. Thermal characterization of rice starches: A polymeric approach to phase transitions of granular starch. *J. Agric. Food Chem.* 34:6.
- Blanshard, J. M. V. 1987. Starch granule structure and function: A physicochemical approach. Page 17 in: *Starch: Properties and Potential*. T. Galliard, ed. Wiley: New York.
- Bowler, P., Williams, M., and Anglold, R. 1980. A hypothesis for the morphological changes which occur on heating lenticular wheat starch in water. *Starch* 32:186.
- Bras, W., Derbyshire, G. E., and Devine, A. 1995. The combination of thermal analysis and time-resolved X-ray techniques—A powerful method for materials characterisation. *J. Appl. Cryst.* 28:26.
- Buleon, A., and Tran, V. 1990. Systematic conformational search for the branching point of amylopectin. *Int. J. Biol. Macromol.* 12:345.
- Buttrose, M. S. 1962. Influence of environment on the shell structure of starch granules. *J. Cell Biol.* 14:159.
- Buttrose, M. S. 1963. Electron microscopy of acid-degraded starch granules. *Stärke* 15:85.
- Cameron, R. E., and Donald, A. M. 1992. A SAXS study of the annealing and gelatinisation of starch. *Polymer* 33:2628.
- Cooke, D., and Gidley, M. J. 1992. Loss of crystalline and molecular order during starch gelatinisation: Origin of the enthalpic transition. *Carbohydr. Res.* 227:103.
- Donald, A. M., and Windle, A. H. 1992. *Liquid Crystalline Polymers*. CUP: Cambridge, UK.
- Donovan, J. 1979. Phase transitions of the starch water system. *Biopolymers* 18:263.
- Donovan, J., and Mapes, C. 1980. Multiple phase transitions of starches and Nägeli amylopectins. *Starch* 32:190.

- French, D. 1984. Organisation of starch granules. Page 183-247 in: *Starch: Chemistry and Technology*. R. L. Whistler, J. N. BeMiller, and E. F. Paschall, eds. Academic Press: London.
- Galliard, T., and Bowler, P. 1987. Morphology and composition of starch. Pages 55-78 in: *Starch Properties and Potential*. CRAC Vol. 13. T. Galliard, ed. John Wiley and Sons: New York.
- Gidley, M. J., and Cooke, D. 1991. Aspects of molecular organization and ultrastructure in starch granules. *Biochem. Soc. Trans.* 19:551.
- Higgins, J. S., and Benoit, H. C. 1996. *Polymers and Neutron Scattering*. Clarendon Press: Oxford, UK.
- Hill, R. D., and Dronzek, B. L. 1973. Scanning electron microscopy studies of wheat, potato and corn during gelatinisation. *Stärke* 25:367.
- Hizukuri, S. 1986. Polymodal distribution of the chain length of amylopectins and its significance. *Carbohydr. Res.* 147:342.
- Hizukuri, S., Kaneko, T., and Takeda, Y. 1983. Measurement of the chain length of amylopectin and its relevance to the origin of crystalline polymorphism of starch granules. *Biochim. Biophys. Acta* 760:188.
- Imberty, A., and Perez, S. 1988. A revisit to the 3d structure of B type starch. *Biopolymers* 27:1205.
- Imberty, A., Chanzy, H., and Pérez, S. 1987. New three-dimensional structure for A-type starch. *Macromolecules* 20:2634.
- Jenkins, P. J. 1995. X-ray and neutron scattering studies of starch granule structure. PhD thesis. Cambridge University: Cambridge, UK.
- Jenkins, P. J., and Donald, A. M. 1996. Applications of small angle neutron scattering to the study of starch granule structure. *Polymer* 37:5559.
- Jenkins, P. J., and Donald, A. M. 1998. Gelatinisation of starch: A combined SAXS/WAXS/SANS study. *Carbohydr. Res.* 308:133.
- Jenkins, P. J., Cameron, R. E., and Donald, A. M. 1993. A universal feature in the structure of starch granules from different botanical sources. *Stärke* 45:417.
- Jenkins, P. J., Cameron, R. E., and Donald, A. M. 1994. In situ simultaneous small and wide angle X-ray scattering: A new technique to study starch gelatinisation. *J. Polym. Sci. Phys. Ed.* 32:1579.
- Koizumi, K., Fukuda, M., and Hizukuri, S. 1991. Estimation of the distribution of chain length of amylopectins by high-performance liquid chromatography with pulsed amperometric detection. *J. Chromatography* 585:233.
- Liu, H., Lelievre, J., and Ayong-Chee, W. 1991. A study of starch gelatinisation using differential scanning calorimetry, X-ray and birefringence measurements. *Carbohydr. Res.* 210:79.
- Perry, P. A. 1999. Plasticisation and thermal modification of starch. PhD thesis. Cambridge University: Cambridge, UK.
- Perry, P. A., and Donald, A. M. 2000a. The role of plasticisation in starch granule assembly. *Biomacromolecules* 1:424.
- Perry, P. A., and Donald, A. M. 2000b. SANS study of the distribution of water within starch granules. *Int. J. Biol. Macromol.* 28:31.
- Robin, P. J. P., Mercier, C., and Duprat, F. 1975. Amidons lintnerises. *Stärke* 27:36.
- Simmons, S., Weigand, C. E., and Albalak, R. J. 1992. Thermoplastic processing of starch: Melt-spinning of starch-based fibers. *Fundamentals of Biodegradable Materials and Packaging*. Wiley: New York.
- Slade, L., and Levine, H. 1989. A food polymer science approach to selected areas of starch gelatinization and retrogradation. Pages 215-270 in: *Frontiers in Carbohydrate Research, I. Food Applications*. R. P. Milane, J. N. BeMiller, and R. Chandrasekaran, eds. Elsevier Applied Science: London.
- Tomka, I. 1991. Thermoplastic starch. Page 627 in: *Water Relationships in Starch*. H. Levine and L. Slade, eds. Plenum: New York.
- Waigh, T. A. 1997. The structure and side chain liquid crystalline polymeric properties of starch. PhD thesis. Cambridge University: Cambridge, UK.
- Wakelin, J. H., Virgil, H. S., and Crystal, E. 1959. Development and comparison of two X-ray methods for determining the crystallinity of cotton cellulose. *J. Appl. Phys.* 30:1654.
- Wang, T., Bogracheva, T., and Hedley, C. 1998. Starch: As simple as A, B, C? *J. Exper. Bot.* 49:481.
- Whistler, R. L., BeMiller, J. N., and Paschall, E. F. 1984. *Starch Chemistry and Technology*. Academic Press: London.
- Yamaguchi, M., Kainuma, K., and French, D. 1979. Electron microscopic observations of waxy maize starch. *J. Ultrastructure Res.* 69:249.

[Received January 2, 2001. Accepted February 12, 2001.]